THERMOCHEMICAL CYCLES FOR H_2 AND CO PRODUCTION: SOME FUNDAMENTAL ASPECTS.

Eric N. Coker, Mark A. Rodriguez, Andrea Ambrosini and James E. Miller

Sandia National Laboratories, PO Box 5800, Albuquerque, New Mexico 87185-1349, USA

Tel. +1 505 272 7593; encoker@sandia.gov

Abstract

Hydrogen and carbon monoxide may be produced using solar-thermal energy in two-stage reactions of water and carbon dioxide, respectively, over certain metal oxide materials. The two-stage process involves thermal reduction of the metal oxide (releasing oxygen), followed by re-oxidation of the metal oxide by either water or carbon dioxide. The most active materials observed experimentally for these processes are complex mixtures of ferrite supported on zirconia based solids, and it is not clear to what extent the ferrites, the zirconia, or a solid solution between the two each participate in the change of oxidation state during the cycling. Identification of the key phases in the redox material that enable splitting of water or carbon dioxide is of paramount importance to developing a working model of the materials. In-situ characterization of reactive materials has been conducted in order to follow phase changes and identify the phases active for splitting, as well as to gain insight into the kinetics of the processes. For the work described here, cobalt-substituted ferrites were prepared by co-precipitation followed by annealing at 1400 °C. An in-situ X-ray diffraction capability was developed and tested, allowing phase monitoring in real time during thermochemical redox cycling. Key observations made for an un-supported cobalt ferrite include: 1) ferrite phases partially reduce to wüstite upon heating to 1400 °C in helium; 2) exposing the reduced material to air at 1100 °C causes immediate re-oxidation; 3) the re-oxidized material may be thermally reduced again at 1400 °C under inert; 4) exposure of a reduced material to CO_2 results in gradual re-oxidation at 1100 °C, but minimization of background O_2-levels is essential; 5) even after several redox cycles, the lattice parameters of the ferrites remain constant, indicating that irreversible phase separation (cobalt from iron) does not occur, at least over the first five cycles. Thermogravimetric analysis under thermal reduction and simulated water-reoxidation and carbon dioxide-reoxidation corroborated the X-ray diffraction data, revealing slow reduction (1400 °C) and slow re-oxidation (1100 °C) of the ferrite.

Keywords: Thermochemical cycle; ferrite; cobalt-ferrite; wüstite; high-temperature XRD; thermal reduction.

1. Introduction

Solar driven two-step ferrite ($A_xFe_{3-x}O_4$) thermochemical cycles are promising as a method for producing H_2 and CO via H_2O- and CO_2-splitting. [1,2,3] The basic cycles consist of a thermal reduction step (TR; reaction (1)) in which solar thermal energy reduces Fe^{III} to Fe^{II}, i.e., spinel transforms to wüstite, followed by a water-splitting step (WS; reaction (2)), or CO_2-splitting step (CDS; reaction 3) wherein the ferrite spinel is regenerated:

$$A_xFe_{3-x}O_4 \rightarrow xAO + (3-x)FeO + 0.5\ O_2 \quad (1)$$

$$xAO + (3-x)FeO + H_2O \rightarrow A_xFe_{3-x}O_4 + H_2 \quad (2)$$

$$xAO + (3-x)FeO + CO_2 \rightarrow A_xFe_{3-x}O_4 + CO \quad (3)$$

Hydrogen production using Fe_3O_4, originally proposed by Nakamura, [4] is not practical since the TR requires 1800 °C resulting in sintering or fusion that must be undone to activate the material for successive cycles; supporting Fe_3O_4 on zirconia or yttria-stabilized zirconia (YSZ) reduces this problem. [5,6] Alternative redox systems where $A \neq Fe$ enable reduced temperature TR, e.g., A = Mn, Co, Ni, Zn, and are now receiving considerable attention. [7] The TR reaction can be driven as low as 1100 °C, although kinetics usually dictate that temperatures above 1300 °C are used, which are readily achievable using concentrated solar-thermal energy. Yields of H_2 and CO are maximized in the range 1080 – 1230 °C; equilibrium concentrations of H_2 and CO would be higher at lower temperatures, but again the reaction kinetics call for the higher temperatures. The need for large temperature swings as well as spatial/temporal

isolation of the TR and WS/CDS reactions (to avoid energetic re-combination of O_2 and H_2/CO) was addressed in the design of the CR5 reactor, described elsewhere. [8] The work described here focuses on some of the materials fundamentals in an effort to understand reaction pathways and enable efficient H_2 and CO production using the CR5.

While it is known that the ad-mixing of a high temperature-stable support, such as ZrO_2, or YSZ to the ferrite is necessary in order for the process to be cyclable, [9] we chose the unsupported ferrite for these initial experiments in order to simplify characterization. Ongoing experiments utilize ferrite materials supported on YSZ and ZrO_2. The current work has probed the complex behavior of ferrites which is not well-defined at high temperatures and under redox conditions, with particular emphasis on phase evolution during thermal processing. The principal techniques employed include high-temperature X-ray diffraction (HT-XRD) and thermogravimetric analysis (TGA) under conditions simulating TR/WS and TR/CDS reactions.

2. Experimental Details

2.1. Materials Synthesis

Cobalt ferrite-based materials with the nominal composition $Co_{0.95}Fe_{2.05}O_4$ were prepared via conventional co-precipitation from a solution of iron nitrate and cobalt nitrate by addition to an ammonia solution. The obtained powders were washed and dried, then calcined to 1100 °C, and then to 1400 °C in air prior to evaluation. This composition was chosen based on results of thermodynamic modeling of phase formation and stability as a function of spinel composition, temperature, and gas composition. [10] The modeling results suggested that Co : Fe ratios between 0.95 : 2.05 and 1.0 : 2.0 offer the optimal spinel fraction in the material, while minimizing the formation of additional iron or cobalt phases.

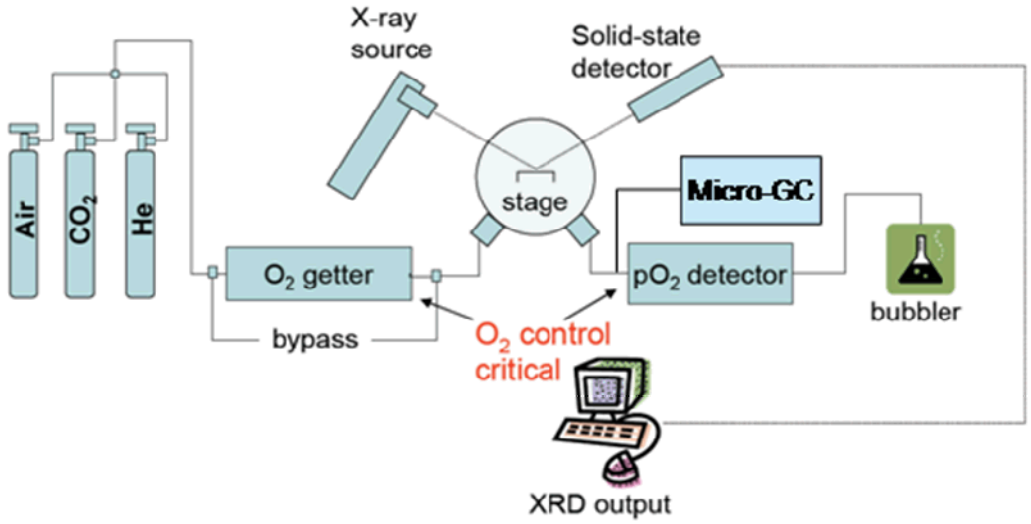

Figure 1. Schematic representation of HT-XRD experimental set-up

2.2. Characterization

High temperature XRD experiments were performed using a Scintag PAD X diffractometer (Thermo Electron Inc.; Waltham, MA). This diffractometer is equipped with a sealed-tube source (Cu K_α, $\lambda = 0.15406$ nm), an incident-beam mirror optic, a peltier-cooled Ge solid-state detector, and a Buehler hot-stage with Pt/Rh heating strip and surround heater. The hot stage lies within a sealed cell with X-ray-transparent beryllium windows, and is operable from ambient temperature to 1600 °C, and at gas pressures from 10^{-9} to 10^3 Torr. An all-metal gas manifold was attached to the inlet of the reaction cell allowing the controlled flow of helium, air, or carbon dioxide through the cell. An oxygen getter furnace (Centorr TM 1B) was installed

in the helium inlet line to remove trace levels of oxygen, and an oxygen- and moisture-specific adsorbent purifier bed was used in the CO_2 line. An oxygen analyzer (Ametek CG1000) attached to the exit line from the cell monitored the oxygen background when running He or CO_2. A micro-gas chromatograph (micro-GC, Agilent Technologies 3000A) was installed in parallel with the oxygen analyzer to allow gas composition monitoring (e.g., evolution of O_2 during TR and evolution of CO during CDS). Samples were analyzed as thin layers (ca. 50 – 100 μm) of powder on top of 10mm x 10mm x 0.5mm high-purity poly-crystalline alumina plates. In-situ HT-XRD experiments were conducted at atmospheric pressure, under gas flow rates of 150 ml min^{-1} (corrected to STP). Figure 1 shows a schematic representation of the HT-XRD system. For the study of phase transformations during TR/CDS cycling, the reaction cell was typically purged with He, heated stepwise to 1400 °C under He, held at 1400 °C under He for 2 hours, stepped down to 1100 °C under He, then exposed to CO_2 at 1100 °C for 5 hours, or until no further change in XRD pattern was observed. Step sizes were typically 50 °C between 800 and 1400 °, and were 100 or 200 °C at lower temperatures. Diffraction patterns were recorded at each step during a 30 minute isothermal hold. Heating and cooling ramp rates were set to 20 °C min^{-1}. Using this experimental set-up, phase fractions as low as ~ 1 wt.-% could be reliably detected. The temperature calibration was performed using the thermal expansion behavior of known materials (e.g., alumina or platinum) to an accuracy of ±5 °C. Diffraction patterns were collected at 40 kV and 30 mA using fixed slits over a scan range of 20 – 80 °2θ at a step-size of 0.04 °2θ and a count time of 1 s. Typical scans were collected in ~30 minute increments.

Room temperature XRD patterns were recorded on either a PAnalytical X-Pert Pro diffractometer, or a Siemens D500 diffractometer using Cu K_α radiation.

Thermogravimetric Analysis/Differential Thermal Analysis (TGA/DTA) was performed on a TA Instruments Q600 SDT. Powder samples were run under simulated solar reduction conditions (Ar/1400 ºC) and oxidizing conditions (air, CO_2, or H_2O/1100 ºC).

3.0. Results and Discussion

3.1. Phases present during TR/CDS over cobalt ferrite

As-prepared cobalt-ferrite materials, with the nominal composition $Co_{0.95}Fe_{2.05}O_4$, exhibited an XRD pattern characteristic of a spinel, with no detectable impurities. Upon heating to 1400 °C under He, partial reduction of the spinel (Fe^{III}/Fe^{II}) to wüstite ($Fe^{II}O$) was observed by XRD, beginning at around 1000 °C, and the wüstite persisted on cooling to 1100 °C (Figure 2). The displacement of diffraction peaks to smaller angles upon heating, and to larger angles upon cooling in Figure 2 is consistent with the thermal expansion and contraction of the lattice, respectively. On exposure to CO_2 with a relatively high O_2-content of ~ 10 – 80 ppm at 1100 °C, a fairly rapid re-oxidation of the wüstite to the spinel occurred during the first hour, followed by a more gradual re-oxidation. No other phases were detected in the course of the experiment; since separate iron- and cobalt-containing phases were not detected, it is assumed that the iron oxide and cobalt oxide constituents remained in solid solution throughout the processing. Post-mortem XRD under ambient conditions after five hours exposure to CO_2 at 1100 °C revealed a residual wüstite content of ~2%. Figure 3 shows a series of consecutive XRD scans taken from Figure 2, and the rapid disappearance of wüstite upon exposure to CO_2 is evident. Note that in scan B (first scan after switching to CO_2 flow), the (111) peak of wüstite was present at approximately the same intensity as in scan A, but the (200) peak had disappeared. The time elapsed between the measurement of the (111) peak and the (200) peak is about two minutes. The results of Figure 3 may be explained by 1) the time lag between beginning CO_2 flow and it reaching the sample (allowing the (111) peak to be registered in scan B, while the (200) peak was measured after CO_2 had reached the sample), and 2) the rapid initial re-oxidation of the wüstite phase, presumably a surface-reaction, resulting in the decrease in intensity of the (200) wüstite peak in scan B. The subsequent, gradual decrease in intensity of the wüstite (111) peak from scan B to scan F is attributed to a relatively slow bulk reaction process, i.e., re-oxidation of wüstite below the surface layers of the grains. The small residual quantity of wüstite observed at the end of this experiment amounted to ~ 1 wt.-% of the sample.

The XRD data in Figure 4 show the progress of an experiment involving TR at 1400 °C, followed by CDS at 600 °C. The phase evolution during TR was similar to that observed in Figure 2, viz. formation of wüstite at

the expense of ferrite beginning at around 1000 °C. The wüstite phase persisted at 600 °C in the low-O_2 environment, and re-oxidation to ferrite upon exposure to CO_2 was noticeably slower than at 1100 °C. Both the (111) and (200) peaks for wüstite remained during the five-hour soak at 600 °C under CO_2; in fact this sample retained ~ 4 % wüstite, as determined by post mortem XRD (Table 1).

The lattice parameters of samples after various TR/CDS protocols were evaluated, and were found to vary by at most 0.005Å between samples, indicating that while the ferrite undergoes a phase change at high temperature, the sample does not change significantly in composition (Table 1). Also, the spinel lattice parameter did not vary even when there was significant wüstite phase fraction remaining upon cool down. This implies that the reduced phase was similar in Fe:Co ratio to the ferrite and would return to its original ferrite lattice upon re-oxidation, as corroborated by recent thermodynamic modeling. [10]

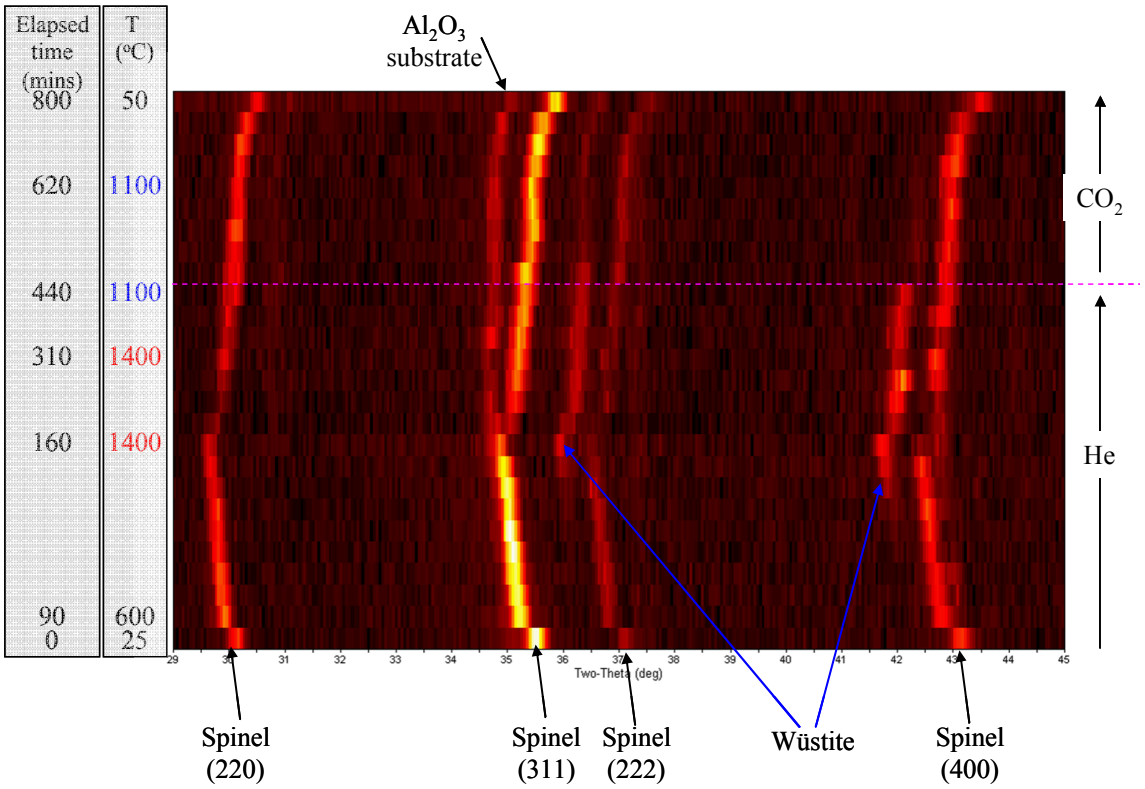

Figure 2. XRD intensities as function of temperature, environment, and time for $Co_{0.95}Fe_{2.05}O_4$. TR at 1400 °C; CDS at 1100 °C.

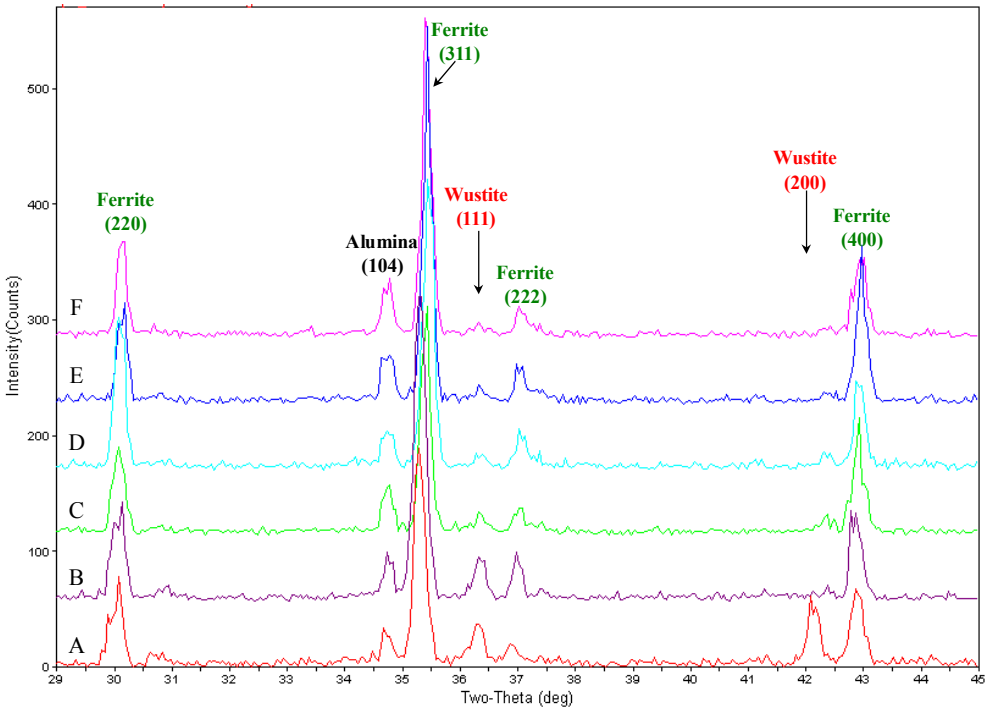

Figure 3. XRD patterns extracted from Figure 2 illustrating fast and slow oxidation processes on switching from He flow (scan A) to CO_2 flow (scans B – F). All scans were collected at 1100 °C.

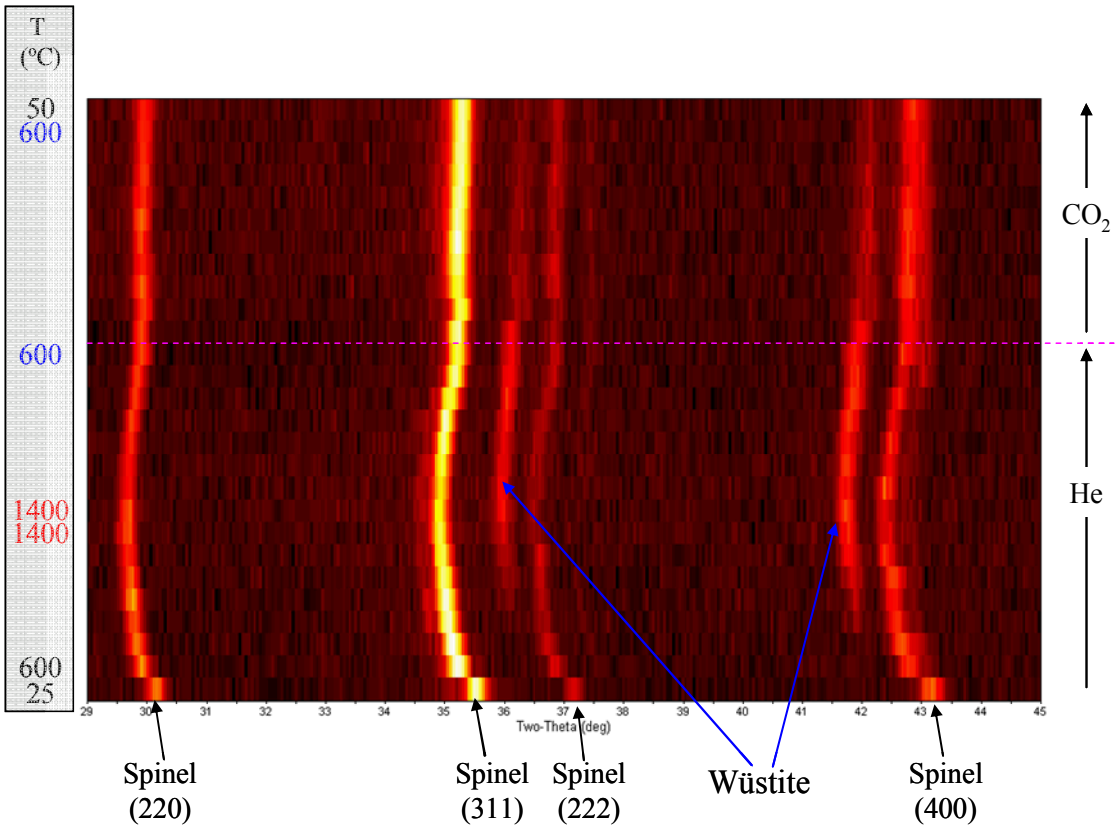

Figure 4. XRD intensities as function of temperature and environment for $Co_{0.95}Fe_{2.05}O_4$. TR at 1400 °C; CDS at 600 °C.

Sample*	Ferrite lattice parameter (Å)	Ferrite wt. fraction (%)	Wüstite lattice parameter (Å)	Wüstite wt. fraction (%)
Before thermal cycling	8.377(2)	100		0
TR 1400 °C Air oxidation 1100 °C	8.382(2)	100		0
TR 1400 °C CDS 1100 °C (80 ppm O_2)	8.378(2)	99		~1
TR 1400 °C CDS 1100 °C (< 10 ppm O_2)	8.381(2)	98	4.258	2
TR 1400 °C CDS 600 °C (< 10 ppm O_2)	8.379(2)	96	4.262	4

Table 1. Phase composition and lattice parameters from XRD before and after thermochemical cycling.

3.2. Kinetics of TR/CDS and TR/WS over cobalt ferrite

The data in Figures 2 – 4 and Table 1 show that the rate of CDS was relatively slow at 1100 °C, and even slower at 600 °C, provided adequate control over background O_2-levels was achieved. Exposure of a thermally reduced sample to air at 600 or 1100 °C caused almost immediate re-oxidation of the wüstite fraction of the material to the spinel, suggesting that it is the decomposition of CO_2 which controls the rate of re-oxidation of wüstite to the spinel during CDS, not a fundamental limit to the rate of oxidation itself and the coupled transport processes. That is, there is reasonable certainty that transport within the bulk is not the principal rate limiting factor. This is consistent with bench reactor tests that also showed that the TR, WS, and CDS reactions are relatively slow, and that the initial stages of TR (O_2 release) are more rapid than the initial stages of WS or CDS (H_2 or CO evolution). [11]

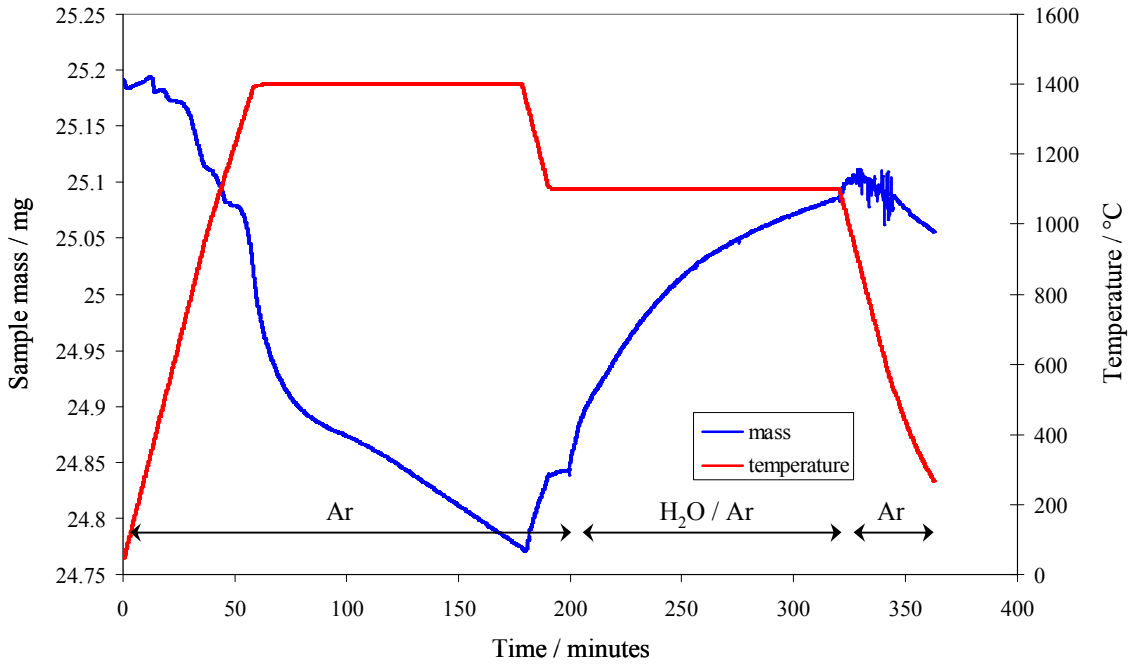

Figure 5. TGA data as function of temperature and environment for $Co_{0.95}Fe_{2.05}O_4$ under TR (Ar) and WS (H_2O/Ar) conditions.

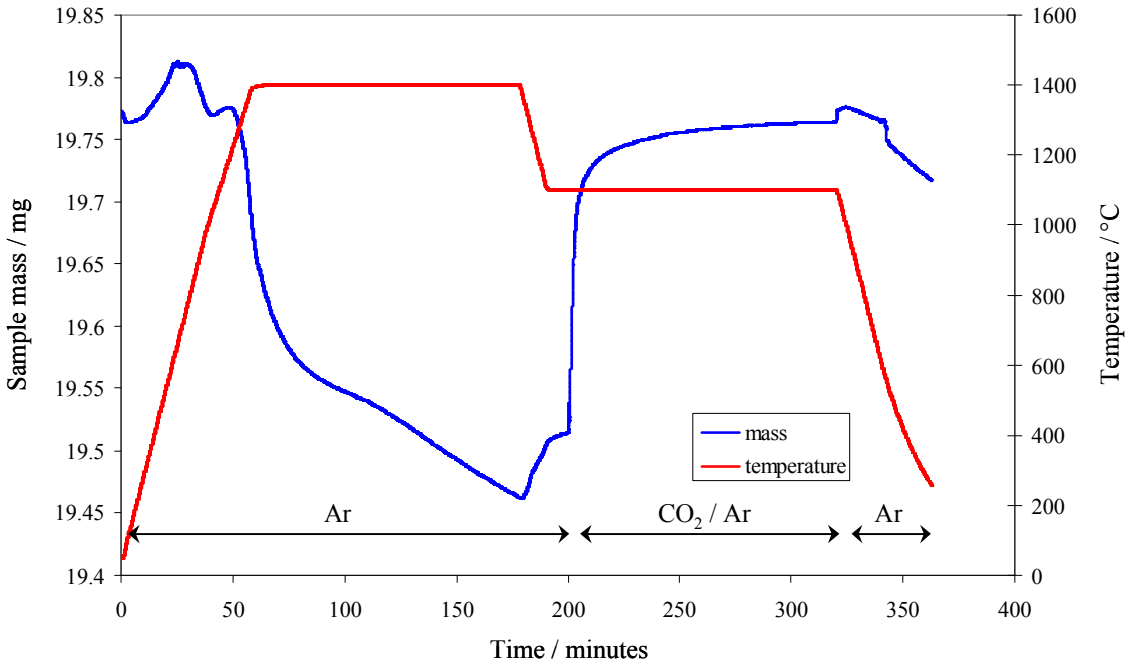

Figure 6. TGA data as function of temperature and environment for $Co_{0.95}Fe_{2.05}O_4$ under TR (Ar) and CDS (CO_2/Ar) conditions.

TGA was performed on $Co_{0.95}Fe_{2.05}O_4$ samples under simulated WS and CDS conditions (Figures 5 and 6). The samples were heated to 1400 °C under Ar gas at a rate of 20 °C min^{-1}, held isothermally for approximately 2 hrs, cooled to 1100 °C, and exposed to either water vapor (approximately 34% RH) in Ar or CO_2 (19.95% in Ar balance) over 2 hrs. The concentrations (ppm) of CO_2 and water vapor in the Ar were calculated to be similar to one another.

Both experiments showed the expected reduction under Ar at 1400 ºC, though it is worth noting that the kinetics were quite slow. The rate of TR was relatively fast for the first 30 minutes, and then became slow; after a reaction time of 2 hours at 1400 °C mass loss due to oxygen evolution was still occurring at a slow rate. The oxidation reactions were considerably faster than TR. The oxidation by CO_2 occurred almost instantaneously, while that by H_2O was slower. This may have been caused in part to the inherently longer time taken for the system to come to equilibrium when switching from Ar to water vapor than the time taken when switching from Ar to Ar/CO_2. However, it is also worth noting that the CDS reaction (Figure 6) exhibited both fast and slow reactions, while the WS reaction (Figure 5) appeared to be governed by a single rate constant. Due to the faster CDS reaction, the magnitude of oxidation via CO_2 was larger than that by H_2O over the course of the 2 hour reaction. Post-mortem XRD of the TGA samples showed no presence of wüstite, unlike those from the in-situ XRD experiments (Table 1). It is possible that a small ingress of air into the TGA system may have occurred, causing the very rapid weight gain during CDS (Figure 6), and forcing the conversion of all of the wüstite phase to ferrite.

The fact that the TR reaction exhibited fast (surface) and slow (bulk) rates, yet the WS reaction did not (Figure 5) may indicate that the reaction between adsorbed H_2O and the wüstite phase occurs at a slower rate than the diffusion of oxygen or metallic species through the ferrite (i.e., bulk – surface interchange). This same argument probably applies to the reaction with CO_2, although the (assumed) oxygen ingress in the CDS experiment (Figure 6) precludes verification of this postulation.

In situ investigations via HT-XRD and TGA of TR, WS, and CDS over cobalt-ferrites supported on YSZ, and other metal oxide systems, will be reported separately. [12]

5. Conclusions

Both WS and CDS can be achieved at 1100 °C over thermally reduced (1400 °C) cobalt-substituted ferrites. The TR, WS, and CDS reactions proceed relatively slowly, due to one or more of: surface reaction kinetics, thermodynamic driving forces, and mass transport to and away from the surface. In-situ XRD allowed the formation of the reduced wüstite phase to be followed between 1000 and 1400 °C (He), as well as the gradual re-oxidation to the ferrite phase upon exposure to CO_2 at 1100 °C. Despite the high temperature phase separations observed, the lattice parameters of samples after various TR/CDS protocols did not change significantly. This implies that the composition of the samples is unchanged and that the wüstite-type Co-Fe phase is similar in Co:Fe ratio as the parent spinel phase. Thermal reduction was found via TGA to occur via an initial relatively fast process, followed by a slow process. These two processes may be attributed to a surface reaction, and a bulk reaction, respectively. The WS reaction, however, appeared to be governed by a single rate constant.

Acknowledgements

This work was funded by the Laboratory Directed Research and Development (LDRD) Office at Sandia National Laboratories. Sandia is a multiprogram laboratory operated by Sandia Corporation, a Lockheed Martin Company, for the United States Department of Energy's National Nuclear Security Administration under contract DE-AC04-94AL85000.

References

1 A. Steinfeld, Solar En. 78, (2005), 603.

2 T. Kodama, Prog. En. Comb. Sci. 29, (2003), 567.

3 J.E. Miller, Sandia Report, SAND2007-8012, (2007), (order at "orders@ntis.fedworld.gov").

4 T. Nakamura, Solar En. 19, (1977), 467.

5 T. Kodama, Y. Nakamuro, T. Mizuno, J. Solar Energy Eng. 128, (2006), 3.

6 T. Kodama, et al., Proceedings of the ASME ISES Conference, Hawaii, 2003.

7 T. Kodama, N. Gokon, Chem. Rev. 107, (2007), 4048.

8 R.B. Diver, J.E. Miller, M.D. Allendorf, N.P. Siegel, R.E. Hogan, J. Solar Energy Eng. 130, (2008), 041001-1.

9 T. Kodama, Y. Nakamuro and T. Mizuno, J. Sol. Energy Eng.-Trans. ASME, 128, (2006), 3-7.

10 M.D. Allendorf, R.B. Diver, N.P. Siegel, J.E. Miller, Energy & Fuels 22, (2008), 4115–4124.

11 J.E. Miller, M.D. Allendorf, R.B. Diver, L.R. Evans, N.P. Siegel, J.N. Stuecker, J. Mater. Sci. 43, (2008), 4714–28.

12 E.N. Coker, M.A. Rodriguez, A. Ambrosini L.R. Evans and J.E. Miller, Chem. Materials, in preparation.